Journal Pre-proof

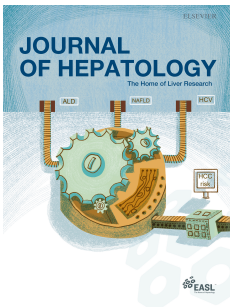

Untargeted lipidomics uncovers lipid signatures distinguishing severe versus moderate forms of acutely decompensated cirrhosis

Joan Clària, Anna Curto, Richard Moreau, Benoit Colsch, Cristina López-Vicario, Juan José Lozano, Ferran Aguilar, Florence A. Castelli, François Fenaille, Christophe Junot, Ingrid Zhang, Maria Vinaixa, Oscar Yanes, Paolo Caraceni, Jonel Trebicka, Javier Fernández, Paolo Angeli, Rajiv Jalan, Vicente Arroyo

PII: S0168-8278(21)01895-X

DOI: https://doi.org/10.1016/j.jhep.2021.06.043

Reference: JHEPAT 8352

To appear in: *Journal of Hepatology*

Received Date: 5 December 2020

Revised Date: 16 June 2021

Accepted Date: 30 June 2021

Please cite this article as: Clària J, Curto A, Moreau R, Colsch B, López-Vicario C, Lozano JJ, Aguilar F, Castelli FA, Fenaille F, Junot C, Zhang I, Vinaixa M, Yanes O, Caraceni P, Trebicka J, Fernández J, Angeli P, Jalan R, Arroyo V, Untargeted lipidomics uncovers lipid signatures distinguishing severe versus moderate forms of acutely decompensated cirrhosis, *Journal of Hepatology* (2021), doi: https://doi.org/10.1016/j.jhep.2021.06.043.

This is a PDF file of an article that has undergone enhancements after acceptance, such as the addition of a cover page and metadata, and formatting for readability, but it is not yet the definitive version of record. This version will undergo additional copyediting, typesetting and review before it is published in its final form, but we are providing this version to give early visibility of the article. Please note that, during the production process, errors may be discovered which could affect the content, and all legal disclaimers that apply to the journal pertain.

© 2021 Published by Elsevier B.V. on behalf of European Association for the Study of the Liver.

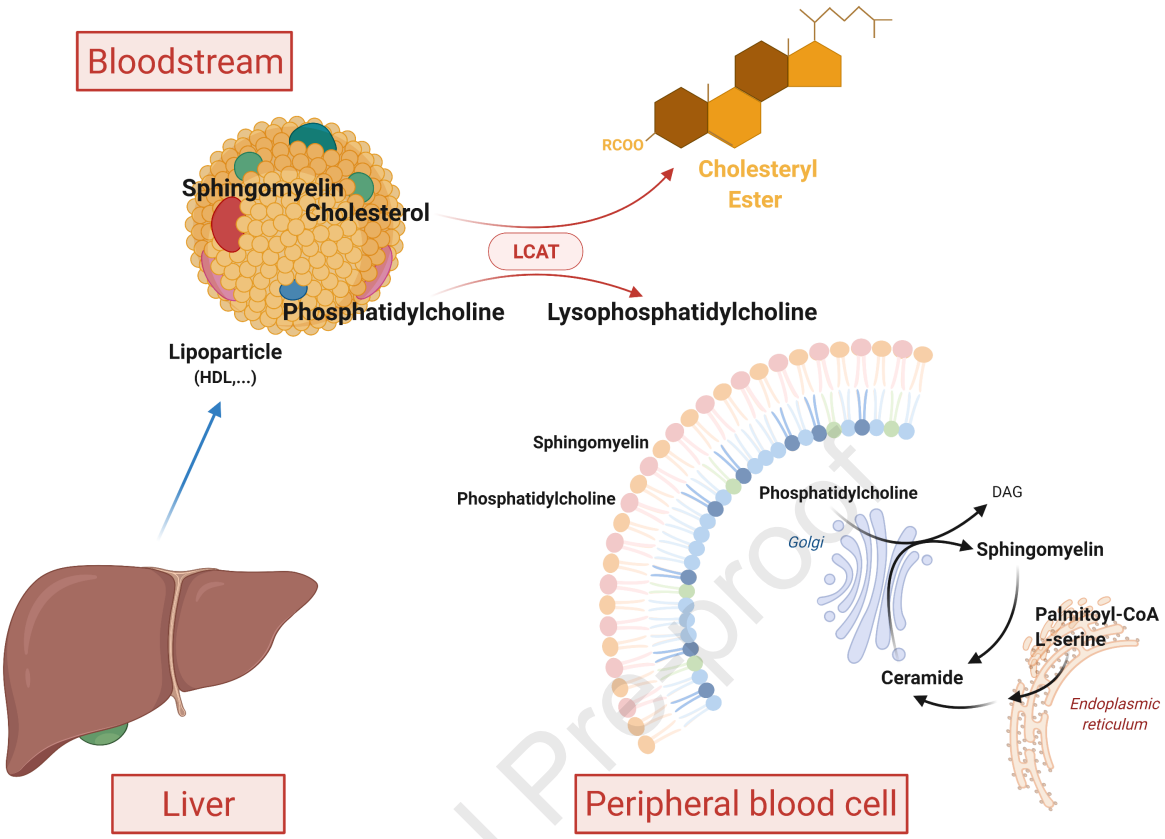

Journal Pre-proof

Journal Pre-proof

Untargeted lipidomics uncovers lipid signatures distinguishing severe versus moderate forms of acutely decompensated cirrhosis

Joan Clària[1,2,3,4,*,†], Anna Curto[1,*], Richard Moreau[1,5,*], Benoit Colsch[6], Cristina López-Vicario[1,2], Juan José Lozano[4], Ferran Aguilar[1], Florence A. Castelli[6], François Fenaille[6], Christophe Junot[6], Ingrid Zhang[1,2], Maria Vinaixa[7,8], Oscar Yanes[7,8], Paolo Caraceni[9], Jonel Trebicka[1,10], Javier Fernández[1,2,4], Paolo Angeli[1,11], Rajiv Jalan[1,12] and Vicente Arroyo[1]

[1]European Foundation for the Study of Chronic Liver Failure (EF Clif) and Grifols Chair, Barcelona, Spain; [2]Hospital Clínic-IDIBAPS, Barcelona, Spain, [3]Universitat de Barcelona, Barcelona, Spain; [4]CIBERehd, Barcelona, Spain; [5]Inserm, U1149, Centre de Recherche sur l'Inflammation (CRI); UMRS1149, Université de Paris; Service d'Hépatologie, Hôpital Beaujon, Assistance Publique-Hôpitaux de Paris, Clichy, France; [6]Université Paris Saclay, CEA, INRAE, Médicaments et Technologies pour la Santé (MTS), MetaboHUB, 91191 Gif-sur-Yvette, France; [7]Metabolomics Platform, Universitat Rovira i Virgili, Tarragona, Spain. [8]CIBERdem, Tarragona, Spain; [9]University of Bologna, Bologna, Italy; [10]JW Goethe University Hospital, Frankfurt, Germany; [11]University of Padova, Padova, Italy; [12]UCL Medical School, Royal Free Hospital, London, United Kingdom.

*Share first authorship

[†]**Corresponding author:** Joan Clària, Hospital Clínic-IDIBAPS, EF Clif, 08036 Barcelona (Spain), tel. +34 932 271 400, e-mail: jclaria@clinic.cat

Keywords: Lipids, lipidomics, decompensated cirrhosis, systemic inflammation, organ failures.

Electronic Word Count: 5,944

Number of Figures/Tables: 7

Data availability: Raw lipidomics data are provided in Supplementary Table 1-2.

Conflict of Interest Statement: The authors declare no competing interests.

Journal Pre-proof

Financial support statement: Our laboratory is supported by the Ministerio de Ciencia e Innovacion (PID2019-105240RB-I00). This study was supported by EF Clif, a non-profit private organization that receives unrestricted donations from Cellex Foundation and Grifols and is partner or contributor in several EU Horizon 2020 program projects (#825694 and #847949). The funders had no influence on the study design, data collection and analysis, decision to publish or preparation of the manuscript.

Author Contributions: Study concept and design (JC, RM, VA); acquisition of metabolomics data (BC, FF, FC, CJ, OY); acquisition of clinical data (PC, JT, JF, PA, RJ); bioinformatics and statistical analysis (AC, JJL, FA, MV); integration of clinical and biological results, interpretation of data and drafting of the manuscript (JC and CLV); revision of the manuscript for important intellectual content (JT, IZ, PA, RJ); study supervision (JC).

Journal Pre-proof

Abstract

Background and Aim: Acutely decompensated of cirrhosis is a heterogeneous clinical entity associated with moderate mortality. In some patients, this condition develops quickly into a more often deadly acute-on-chronic liver failure (ACLF), in which other organs such as the kidneys or brain fail. The aim of this study was to characterize the blood lipidome in a large series of patients with cirrhosis and identify specific signatures associated with acute decompensation and ACLF development.

Methods: Serum untargeted lipidomics was performed in 561 patients with acutely decompensated (AD) cirrhosis (518 without and 43 with ACLF) (discovery cohort) and in 265 AD patients (128 without and 137 with ACLF) in whom serum samples were available to perform repeated measurements during the 28-day follow-up (validation cohort). Analyses were also performed in 78 AD patients included in a therapeutic albumin trial, 43 patients with compensated cirrhosis and 29 healthy subjects.

Results: The circulating lipid landscape associated with cirrhosis was characterized by a generalized suppression, which was more manifest during acute decompensation and in non-surviving patients. By computing discriminating accuracy and the variable importance projection score for each of the 223 annotated lipids, we identified a sphingomyelin fingerprint specific for AD cirrhosis and a distinct cholesteryl ester and lysophosphatidylcholine fingerprint for ACLF. Liver dysfunction, mainly, and infections were the principal net contributors to these fingerprints, which were dynamic and interchangeable between AD patients whose condition worsened to ACLF and those who improved. Notably, blood lysophosphatidylcholine levels increased in these patients after albumin therapy.

Conclusions: Our findings provide insights into the lipid landscape associated with decompensation of cirrhosis and ACLF progression and identify unique noninvasive diagnostic biomarkers of advanced cirrhosis.

Journal Pre-proof

Lay Summary

Analysis of lipids in blood from patients with advanced cirrhosis reveals a general suppression of their levels in the circulation of these patients. A specific group of lipids known as sphingomyelins are useful to distinguish compensated from decompensated patients with cirrhosis. Another group of lipids designated cholesteryl esters further distinguish patients with decompensated patients who are at risk of developing organ failures.

Journal Pre-proof

Journal Pre-proof

Introduction

Patients with acutely decompensated (AD) cirrhosis frequently develop acute-on-chronic liver failure (ACLF), a syndrome associated with organ failures and dysfunctions across the six major organ systems (liver, kidney, brain, coagulation, circulation, and respiration) resulting in high short-term mortality (1,2). Studies reporting that systemic inflammation is a major driver of ACLF and that variations in the blood non-lipid metabolome are associated with its progression (3,4) have advanced our understanding of this syndrome. However, at present, little is known about the characteristics of the blood lipidome in ACLF.

Lipids are recognized not only as source of energy and as essential cellular components involved in organelle homeostasis and cell signaling and survival, but also in the regulation of inter-organ communication and metabolism and especially in governing immune responses (5-7). Indeed, lipids and immune responses are highly integrated, and altered lipid composition interferes with immune regulation in multiple tissues leading to immune-metabolic dysregulation and uncontrolled inflammation (7). In addition, lipids interact with Toll-like receptors triggering inflammation and several lipid mediators are important inflammatory cues acting as intercellular signaling molecules (8,9).

In the current study we performed a comprehensive untargeted lipidomic examination to capture concise blood lipid signatures in patients with AD cirrhosis with and without ACLF prospectively enrolled in the CANONIC study. Changes in the blood lipidome were also monitored in patients with AD cirrhosis receiving human serum albumin (HSA) as therapy. The aims of this investigation were to: 1) characterize the specific lipidome profile associated with AD cirrhosis; 2) assess how the blood lipidome signature changes during ACLF development; 3) ascertain whether there are distinct lipid fingerprints for each type of organ failure in these

patients; and 4) assess the dynamics of the lipid fingerprints during the clinical course and their response to treatment. The overall goal of this study was to describe the lipid landscape associated with decompensation of cirrhosis and progression to ACLF in patients with AD cirrhosis and to identify useful noninvasive biomarkers of the entire spectrum of end-stage liver disease.

Journal Pre-proof

Experimental procedures

Study Participants

The investigation used biobanked serum samples from 826 patients with AD cirrhosis from the CANONIC study (1), who were split into a discovery cohort (n=561, including 43 patients with ACLF) and a validation cohort (n=265, including 137 patients with ACLF). The latter group was composed of patients in whom serum samples were available to perform repeated measurements during the 28-day follow-up. This strategy allowed cross-sectional and longitudinal validation of the findings. The investigation also included samples from 29 healthy subjects (HS), 43 patients with compensated cirrhosis (CC) and 78 patients with AD cirrhosis receiving HSA as therapy from the INFECIR-2 study (10). For simplification purposes, the groups of patients with AD cirrhosis with and without ACLF were named AD-ACLF and AD-no ACLF, respectively. Complete details are given in Box 1 and supplementary information.

Analysis of lipids, non-lipid metabolites, gene expression and lecithin-cholesterol acyl transferase (LCAT) levels.

Lipidomic and metabolomic analyses were performed by liquid chromatography coupled to high-resolution mass spectrometry (LC-HRMS) and LC−MS and MS/MS. For lipidomics, internal standards representative of each lipid class were used to monitor the extraction recovery and validate the data treatment process. Box 2 defines the abbreviations of the most common lipid classes. Gene expression was determined by real-time polymerase chain reaction and plasma LCAT levels by ELISA (see supplementary information).

Statistical analysis

Journal Pre-proof

We performed multivariate models, including age and gender and computed the area under the receiver-operating-characteristic curve (AUC) to estimate the value of each lipid to discriminate the study groups. Then, AUC values were used for unsupervised hierarchical cluster analysis.

The partial least squares discriminant analysis (PLS-DA) model was also used to maximize inter-class variance and to compute the variable importance projection (VIP) score for each lipid. See supplementary information for full details.

Journal Pre-proof

Results

Table 1 shows the baseline clinical and standard laboratory data of the discovery cohort. C-reactive protein and cytokine levels were significantly higher in patients with AD-no ACLF relative to CC and much higher in AD-ACLF relative to AD-no ACLF, indicating a full-blown state of systemic inflammation in patients with AD-ACLF.

Suppression of blood lipid levels parallels disease severity

The untargeted lipidomics analysis unambiguously identified 223 lipid species in serum of patients with cirrhosis at any stage and HS (**Table S1**). To reduce the dimension of this dataset, we performed unbiased principal component analysis (PCA). A general clustering trend from HS to CC to AD-ACLF was observed along PC1/PC2 scores plot gathering 74% of the total variance with the progression to AD-ACLF being the major contributor to variation of circulating lipids (**Figure S1A-B**, **Table S2**). Next, we explored the relationship between the study groups and the underlying patterns of blood lipid levels by performing a supervised two-way cluster analysis. As shown in **Figure 1A** and **Figure S1C**, the levels of most lipid families were similar in CC and HS and decreased, except for fatty acids (FAs), in both the AD-no ACLF and AD-ACLF groups, indicating that the variation in the blood lipidome associated with decompensated cirrhosis is primarily characterized by a generalized reduction in blood lipids. This pattern is further illustrated in **Figure 1B**, in which levels for each lipid were compared in a pairwise fashion between CC, AD-no ACLF and AD-ACLF with respect to HS and their fold changes ranked in a Cleveland plot. The zoomed-in plots revealed that the monounsaturated FA (MUFA) palmitoleic acid (16:1) together with phosphatidylcholines (PCs) containing MUFAs ranked in first place as the more abundant lipids in AD-no ACLF and AD-ACLF patients (**Figure 1B**, top right). On the other hand, cholesteryl esters (CEs) and lysoPCs (LPCs) containing the omega-3-polyunsaturated FAs (PUFAs) eicosapentaenoic acid

(EPA, 20:5) and docosahexaenoic acid (DHA, 22:6), respectively, ranked first among the lipids with the greatest reductions (**Figure 1B**, bottom right). Of note, for each lipid species, the reduction in AD-ACLF was greater than the corresponding reduction in the other groups of patients. These results are also illustrated using volcano plots with each lipid family coded with a different color (**Figure 1C).**

We next created a supervised clustered correlation matrix of lipids within patients with cirrhosis at any disease stage, including 8 non-lipid metabolites and 18 cytokines/chemokines/macrophage markers in these analyses. In general there was a positive correlation among the lipids, except for FAs, which showed a positive correlation with themselves but inverse relationships with the remaining lipids (**Figure 1D**). In contrast, lipids showed weak negative correlations with non-lipid metabolites and inflammatory markers, except for very modest positive correlations between triglycerides, FAs and some PCs with interleukin-8, pentose phosphates and D-galacturonic and D-glucuronic acids (**Figure 1D**, **Figure S2A**). We finally transformed the lipid-lipid correlation matrix into a network where nodes represented individual lipid species that had at least one significant correlation (rho>0.8) with other lipids. As shown in **Figure S2B**, the correlation network of lipids in patients with cirrhosis (at any stage of the disease) is displayed circularly, similarly to that previously described in human and murine cells (11). We also compared the appearance of the circular networks between AD-no ACLF and CC and between AD-no ACLF and AD-ACLF and color-coded each node in the network according to the fold change (red: increase, blue: decrease) (**Figure S2C**). This analysis confirmed that the most common feature observed in AD-no ACLF and AD-ACLF was a generalized suppression of blood lipid levels, these changes being more evident during transition from CC to AD-no ACLF than during the development of ACLF.

Journal Pre-proof

Identification of a lipid fingerprint specific for AD-no ACLF

We next explored whether any combination or combinations of lipids could serve as a fingerprint to discriminate AD-no ACLF from CC. To address this, we computed the AUC for each of the 223 lipids to assess its discriminating accuracy between AD-no ACLF and CC. This analysis identified three clusters: cluster 1 composed of 55 lipids with high significant association with AD-no ACLF (AUCs between 0.65-0.89) and clusters 2 and 3, which included 68 and 100 lipids, respectively, less associated with AD-no ACLF (**Figure 2A**). The lipids included in cluster 1 ranked by AUCs and P values are listed in **Table S3** and also shown in **Figure 2A**. The lipid fingerprint was practically identical when the AUCs were computed considering only the group of patients without any organ dysfunction ("mere AD-no ACLF") (see definitions in Box 1), indicating it is intrinsic and specific for AD-no ACLF cirrhosis (**Figure 2A**). Importantly, the levels of all the lipids included in this fingerprint were, without exceptions, markedly reduced in AD-no ACLF as compared to CC and HS (**Figure S3**). Consistent with this, the corresponding eigenlipid (a value representative of the levels of the 55 lipids composing the fingerprint) was reduced in AD-no ACLF (**Figure 2B**). Of note, among the 10 lipids that attained the highest AUCs and lowest P values, there were 6 members of the SM family (SM(d18:1/21:1), SM(d18:1/23:0), SM(d18:1/20:1), SM(d18:1/22:1), SM(d18:1/22:0) and SM(d18:1/21:0)) (**Table S3**).

The lipid fingerprint of AD-no ACLF is associated with liver dysfunction

Since the liver plays a central role in lipid metabolism, we next wondered how the lipid fingerprint would appear in patients of the AD-no ACLF group with single liver dysfunction. The AD-no ACLF fingerprint was remarkably more intense in patients with liver dysfunction than in those without and the changes affected all the lipids independently of whether they were part or not of the fingerprint (**Figure 2C**). Furthermore, the heatmaps were similar in patients

of the AD-no ACLF group with either single liver dysfunction, liver failure or single coagulation failure (which highly depends on altered liver function) (**Figure 2C**). The eigenlipid of the AD-no ACLF fingerprint was significantly lower in patients with single liver dysfunction and liver failure versus mere AD-no ACLF (**Figure 2D**), corroborating that normal liver function is a prerequisite for maintaining blood lipid homeostasis. Furthermore, the intensity of the lipid fingerprint (**Figure 2C)** and the eigenlipid (**Figure 2E**) differed between patients with and without bacterial infections. The eigenlipid was also lower in patients with no infection at inclusion but later developed infection during hospitalization (**Figure S4**), suggesting an interplay between infection, immune responses and lipid homeostasis.

Sphingolipids, in particular SMs, are the best indicators of AD-no ACLF

We next computed the VIP score for each lipid of the fingerprint. This analysis revealed that sphingolipids was the family that attained the best discriminating accuracy between AD-no ACLF and CC (**Figure S5A**). Indeed, by ranking the 20 lipid species with the highest VIP scores, four out of the top 5 positions were assigned to SM(d18:1/23:0), SM(d18:1/20:1), SM(d18:1/22:1) and SM(d18:1/21:1) (**Figure S5B**). Moreover, the 5 lipids with the highest VIP scores matched the 5 lipids with the highest AUCs and P values (**Table S3**). The finding that two different unbiased bioinformatic strategies yielded concurrent results reinforces the view that sphingolipids, and particularly members of the SM family, are the best discriminating factors of AD-no ACLF.

Mechanistic aspects of the SM landscape in AD-no ACLF

To gain deeper understanding of these findings, we explored sphingolipid metabolism in patients with cirrhosis. Sphingolipids are ubiquitous constituents of cellular membranes, and besides their structural role, play a major role in regulating innate and adaptive immune

responses and cell survival (12). **Figure 3A** shows a schematic diagram of the sphingolipid pathway. *De novo* sphingolipid biosynthesis involves the condensation of L-serine with palmitoyl-CoA, the activated form of palmitate, mediated by serine palmitoyltransferases in the endoplasmic reticulum to produce ceramide, which is then transported to the Golgi for the synthesis of SM. Alternatively, SM can be synthesized from PC and ceramide in the Golgi by SM synthases. In our study, the serum concentrations of SM(d18:1/21:1), SM(d18:1/23:0) and PC(37:3), which were the 3 lipids with highest discriminating accuracy for AD-no ACLF (**Table S3**), were significantly reduced in parallel with the severity of the disease (**Figure 3B-C**). In addition, patients with AD-no ACLF had reduced levels of serine and palmitate (starting point of *de novo* biosynthesis) and choline (biosynthesis via PC) (**Figure 3D-F**). Moreover, ceramides, which are both intermediates and derivatives of SM, were markedly suppressed in AD-no ACLF patients (**Figure 3G**). Since SM and ceramide pathways commonly terminate into the formation of the bioactive lipid mediator sphingosine-1-phosphate (13), we next measured serum sphingosine-1-phosphate levels in a subgroup of 80 patients with AD-no ACLF and AD-ACLF. As shown in **Figure 3H**, circulating sphingosine-1-phosphate concentrations were significantly reduced in these patients. We finally monitored the expression of key enzymes of the SM pathway in peripheral blood mononuclear cells from these patients. The expression of genes coding for enzymes involved in SM biosynthesis (*SPLTC1*, *SGMS1* and *SGMS2*) and breakdown (*SMPD1*, *SMPD3* and *SGPL1*) were downregulated in patients with AD cirrhosis (**Figure 3I**, **Figure S6)**. Together, these data evidence a generalized suppression of the sphingolipid pathway in cirrhosis.

Identification of a distinct lipid fingerprint specific for AD-ACLF. Identification of CEs as the best indicators

Journal Pre-proof

Having established the AD-no ACLF fingerprint, we then wondered whether any combination of lipids could serve as an ACLF-specific lipid fingerprint. **Figure 4A** shows the unsupervised hierarchical cluster analysis of the AUCs discriminating patients with AD-ACLF of any grade from patients with mere AD-no ACLF. This analysis identified a subcluster (subcluster A) comprising 17 lipids with a high association with ACLF (AUCs from 0.61 to 0.76 and P values up to $2x10^{-8}$) (**Table S4**). Two members of the CE family showed the highest AUC values in this subcluster, which was also enriched in lysophospholipids, mainly LPCs (**Figure 4A and Table S4**). Importantly, the VIP score analysis confirmed that CEs had the highest discriminant capacity to distinguish AD patients with ACLF from those without (**Figure S7A**). Specifically, among the top 5 positions, four were assigned to CEs containing omega-3 (α-linolenic (18:3)) and omega-6 (linoleic acid (18:2)) PUFAs and the MUFAs oleic (18:1) and heptadecenoic (17:1) acids (**Figure S7B**). Of note, the intensity of subcluster A increased in parallel with the number of organ failures, peaking at ACLF-3, at which AUCs reached maximum values between 0.93-0.98 (**Figure 4A**). The eigenlipid representative of the serum levels of the 17 lipids composing subcluster A progressively decreased from HS to AD-ACLF via CC and AD-no ACLF and across ACLF grades (**Figure 4B-C**). Taken together, these findings indicate that subcluster A can be seen as a lipid fingerprint that characteristically discriminates AD-ACLF from AD-no ACLF.

Liver failure and infection are major determinants of the AD-ACLF lipid fingerprint

We next wondered whether the AD-ACLF lipid fingerprint would be the same for each category of organ failure. To address this, we compared the lipid fingerprint of patients with AD-ACLF of any grade to that of patients with single kidney failure or dysfunction, patients with single liver failure associated with kidney and/or brain dysfunction and patients with liver failure combined with either kidney, brain or coagulation failures (other types or organ failures within

the ACLF spectrum were not scrutinized because of the low number of patients). Liver failure, either alone or in combination with other organ failures, was the most important net contributor to define the specific ACLF lipid fingerprint (**Figure 4D).** The combination of liver and coagulation failures resulted in widespread alteration of lipid homeostasis (**Figure 4D**). In addition, bacterial infections significantly contributed to the assembly of the ACLF fingerprint (**Figure 4E**), reinforcing the view that the circulating lipid profile is also associated with immune response against pathogens.

Pathophysiological aspects related to the CE and LPC landscape in AD-ACLF

To gain deeper understanding of the ACLF lipid fingerprint, we focused on CEs, which was the lipid family with the highest discriminating accuracy between AD-ACLF and AD-no ACLF (**Figure S7A**). **Figure 5A** shows reduced levels of the two CEs with the highest discriminating power. CEs are produced by transfer of a FA from the phospholipid PC to cholesterol on the surface of high-density lipoproteins (HDL), a process that is mediated by LCAT, an enzyme predominantly synthesized in the liver (**Figure 5B**). Consistent with the suppressed levels of CEs, LCAT concentrations followed a downward trend that reached statistical significance in patients with AD-ACLF (**Figure 5C**), accompanied by the accumulation of mevalonate, the intermediate in cholesterol biosynthesis (**Figure S8**). Of note, CE and LPC biosynthetic pathways are intricately connected since the removal of a FA from PC by LCAT to feed CE biosynthesis results in the formation of LPC (**Figure 5B**). Accordingly, an increase in the PC to LPC ratio, and consequently, reduced conversion of PC to LPC was observed (**Figure 5D**). Finally, since serum CEs contain relatively high proportions of PUFA, we calculated the ratio between CEs containing the omega-6-PUFA arachidonic acid (20:4) and CEs containing the omega-3-PUFA EPA (20:5). As shown in **Figure S9**, this ratio had a positive relationship with

the severity of the disease. This is in agreement with the finding that CE(20:5) was the lipid with the highest fold change reduction in AD-ACLF patients (**Figure 1B**).

Validation and dynamics of the AD-no ACLF and AD-ACLF lipid fingerprints

We next confirmed the lipid fingerprints identified in the discovery cohort in a group of 265 patients (128 AD-no ACLF and 137 AD-ACLF) from the CANONIC study in whom samples were available to perform repeated measurements during the 28-day follow-up (**Table S5-S7, Figures S10-S11**). This validation cohort was also useful to investigate the dynamics of the lipid fingerprints during the clinical course (**Table S8**). The lipid levels paralleled the clinical course with a decrease in patients with AD-no ACLF at enrollment whose condition worsened (from mostly reddish to more bluish color) (**Figure S12A)** accompanied by a lower eigenlipid (**Figure S12B**). The AD-no ACLF fingerprint was also intensified in these patients (**Figure 6A**), and SMs were displaced by lipids belonging to the AD-ACLF fingerprint (i.e. CEs and LPCs) from the top ranking AUC positions (**Table S9**). On the other hand, patients with AD-ACLF at enrollment whose clinical status improved to AD-no ACLF or to a lower ACLF grade showed an increase in serum lipid levels (from bluish to more reddish color, **Figure S12C**) without changes in the eigenlipid (**Figure S12D**). In these patients, the AD-ACLF fingerprint was attenuated (**Figure 6B)** and the AUC values of the lipids composing this fingerprint lost their statistically significance to differentiate them from patients without ACLF (**Table S10**). Of interest, the eigenlipids of the AD-no ACLF and AD-ACLF fingerprints were significantly lower in patients not surviving the 28-day follow-up (**Figure 6C-D**), reinforcing previous observations indicating that reduced blood lipid levels are associated with higher mortality (14-16).

Response of blood lipids to HSA therapy

Journal Pre-proof

We finally wondered how the lipid profile would be affected by HSA infusions, which is an effective therapy in the management of patients with AD cirrhosis (17). For this purpose, we performed untargeted LC-MS analysis of plasma samples from patients included in the INFECIR-2 trial, a randomized, controlled, multicenter trial assessing the effect of HSA therapy (10). Preprocessing of the data collected from three different LC-MS ionization modes resulted in the initial detection of 6,862 putative features (2,062 in ESI-, 2,583 in ESI+, and 2,217 in ESI+ pH 9), of which 964 (315 in ESI-, 367 in ESI+ and 282 in ESI+ pH 9) were selected for further MS/MS confirmation. After confirmation analysis, we identified 27 metabolites with differential abundance after HSA treatment, of which 4 showed statistically significance ($p<0.05$) in the paired comparison before and after treatment (**Figure 6E**). Two out of these 4 distinct metabolites were lipids, namely LPC(O-16:0) and LPC(18:3), the levels of which significantly increased in patients receiving HSA therapy (**Figure 6F** and **Figure S13**). For comparison purposes, LPC(O-16:0) levels were also increased in patients of the validation cohort whose condition improved and who survived the 28-day follow-up (**Figure 6G**). Since reduced LPC levels predict survival (14), their specific rise after HSA infusion suggests the utility value of these lipids to monitor the response to therapy in advanced cirrhosis.

Journal Pre-proof

Discussion

This study describes the characteristic blood lipid landscape of patients with AD cirrhosis and of those progressing to ACLF. This study also demonstrates an association between the lipid landscape and the clinical outcomes of these patients. The main findings of our study are the following: first, we describe a generalized suppression of blood lipids as a characteristic feature of patients with AD cirrhosis and ACLF, in whom a decay of plasma lipid levels parallels disease severity. Second, we identify a lipid fingerprint, mainly composed by SMs, specific for AD cirrhosis without ACLF. Third, we demonstrate that AD patients who developed ACLF present a distinct and unique lipid fingerprint mainly composed by CEs. Fourth, we describe that these lipid fingerprints are dynamic and interchangeable depending on the clinical course of the disease. Finally, we provide evidence that the composition of circulating lipids is readjusted in response to HSA therapy.

Our data indicate that a generalized suppression of circulating lipids in patients with AD cirrhosis with and without ACLF is mainly dictated by liver dysfunction. It is widely known that the liver is a key organ in the production of endogenous lipids, apolipoproteins and lipoproteins and that liver dysfunction is linked to a disturbed serum lipid profile (18). For instance, serum concentrations of total, HDL, low-density lipoprotein and very-low-density lipoprotein cholesterol closely reflect the hepatic biosynthetic function (19). However, changes in lipid patterns as well as remodeling of the lipid profile also take place in blood leukocytes in response to differential stimuli, such as pathogens (20). Therefore, our finding that the serum lipid profile differed between patients with bacterial infections and those without, suggests that the circulating lipidome is also influenced, at least in part, by the immune response against pathogens.

The lipid fingerprint in patients with AD cirrhosis without signs of ACLF was primarily characterized by a remarkable suppression in SMs, which are sphingolipids containing a FA, a sphingosine and a phosphocholine or phosphoethanolamine group. Earlier observations demonstrated that lower levels of sphingolipids are associated with poor survival in patients with alcoholic cirrhosis (15) and that dysregulated formation of complex sphingolipids is a characteristic feature of malnutrition in hospitalized patients with AD cirrhosis (21). In addition, circulating extracellular vesicles carrying sphingolipid cargo have been shown to predict survival in decompensated alcoholic cirrhosis (22). Of interest, SM is an abundant sphingolipid species in HDL (23), and therefore the presence of very low levels of HDL particles in patients with AD cirrhosis (24) likely contributes to the presence of reduced levels of these sphingolipids in these patients. On the other hand, the lipid fingerprint in patients with AD cirrhosis and ACLF was primarily characterized by a remarkable suppression in the serum levels of CEs and LPCs. Paradoxically, HDL is also involved in the biosynthesis of CEs in the circulation, and therefore this lipoparticle appears to be instrumental in defining the lipid fingerprints of both AD cirrhosis and ACLF. An interesting aspect to consider is that CEs accumulate in the cells of the adrenal cortex where they are used for the synthesis of steroid hormones (25). Therefore, reduced CE levels could lead to adrenal failure in patients with AD-ACLF, being associated with poor liver function, renal failure, refractory shock, and high mortality in these patients (26). Finally, in our study, LPC levels systematically decreased in patients with cirrhosis in parallel with disease severity. In these patients, LPCs have been reported to predict survival (14). LPCs are lipids with potent immunomodulatory properties that have the ability to reduce tissue and organ injury, ameliorate cytokine secretion and enhance bacterial clearance (27,28). Furthermore, LPC administration has been shown to inhibit LPS- or peptidoglycan/lipoteichoic acid-induced multiple organ damage in rats (29). Therefore, our finding that LPC levels rose after the infusion

of HSA in patients with AD cirrhosis advocates that these lipids are suitable for sensing not only the severity of the disease but also the response to HSA therapy.

Our study has some limitations. For instance, the observational nature of our study does not allow any mechanistic interpretation nor formally derive any causality of the general suppression of blood lipids in AD cirrhosis. In addition, no single lipid but rather a cluster of lipids was identified as an ideal biomarker for the different stages of decompensated cirrhosis. Finally, our study does not provide any information on the interaction of lipids with gene variants associated with liver disease. This is of interest because associations between a single nucleotide polymorphism in lysophospholipid acyltransferase and decreased serum triglycerides and between a variant in mitochondrial amidoxime-reducing component 1 and higher levels of SMs have been reported in patients with chronic liver disease (30,31).

In conclusion, by the characterization of the blood lipid landscape in a large number of patients (n=971 in total), this study provides a comprehensive view of the blood lipid landscape associated with acute decompensation of cirrhosis and progression to ACLF. Lipids are too often neglected in clinical practice, but our study raises awareness on the importance of the lipid composition of enteral or parenteral diets as disease modifying factors in critically ill patients. Finally, the identification of distinct and specific lipid fingerprints for patients with AD cirrhosis and for those with ACLF offers unique noninvasive diagnostic opportunities to characterize the entire spectrum of end-stage liver disease.

Journal Pre-proof

Abbreviations: ACLF: acute-on-chronic liver failure, AD: acute decompensation, CC: compensated cirrhosis, CE: cholesteryl ester, Cer: ceramides, DHA: docosahexaenoic acid, EPA: eicosapentaenoic acid, FA: fatty acid, HDL: high-density lipoprotein; HRMS: high-resolution mass spectrometry, HSA: human serum albumin, LC: liquid chromatography, LCAT: lecithin-cholesterol acyl transferase, LPC: lysophosphatidylcholine, LPE: lysophosphatidylethanolamine, MS: mass spectrometry, MUFA: monounsaturated fatty acid, PCA: principal component analysis, PC: phosphatidylcholine, PE: phosphatidylethanolamine, PI: phosphatidylinositol, PLS-DA: partial least squares discriminant analysis, PS: phosphatidylserine, PUFA: polyunsaturated fatty acid, SM: sphingomyelin, SMT: standard medical treatment, SPTLC: serine palmitoyltransferase; TG: triglyceride, VIP: variable importance projection score

Acknowledgments: We thank the IDIBAPS Biobank for careful assistance in the handling of samples.

Journal Pre-proof

References

1. Moreau R, Jalan R, Ginès P, Pavesi M, Angeli P, Cordoba J, et al. Acute-on-chronic liver failure is a distinct syndrome that develops in patients with acute decompensation of cirrhosis. Gastroenterology 2013;144:1426-1437.

2. Arroyo V, Moreau R, Jalan R. Acute-on-Chronic Liver Failure. N Engl J Med. 2020;382:2137-2145.

3. **Clària J, Stauber RE**, Coenraad MJ, Moreau R, Jalan R, Pavesi M, et al. Systemic inflammation in decompensated cirrhosis. Characterization and role in acute-on-chronic liver failure. Hepatology 2016;64:249-1264.

4. **Moreau R, Clària J,** Aguilar F, Fenaille F, Lozano JJ, Junot C, et al. Blood metabolomics uncovers inflammation-associated mitochondrial dysfunction as a potential mechanism underlying ACLF. J Hepatol. 2020;72:688-701.

5. Phillips R, Ursell T, Wiggins P, Sens P. Emerging roles for lipids in shaping membrane-protein function. Nature 2009;459:379-85.

6. Quehenberger O, Dennis EA. The human plasma lipidome. N Engl J Med. 2011;36:1812-23.

7. Ertunc ME, Hotamisligil GS. Lipid signaling and lipotoxicity in metaflammation: Indications for metabolic disease pathogenesis and treatment. J. Lipid Res. 2016;57:2099–2114.

8. Köberlin MS, Heinz LX, Superti-Furga G. Functional crosstalk between membrane lipids and TLR biology. Curr Opin Cell Biol. 2016;39:28-36.

9. López-Vicario C, Checa A, Urdangarin A, Aguilar F, Alcaraz-Quiles J, Caraceni P, et al. Targeted lipidomics reveals extensive changes in circulating lipid mediators in patients with acutely decompensated cirrhosis. J Hepatol. 2020;73:817-828.

10. **Fernández J, Clària J,** Amorós A, Aguilar F, Castro M, Casulleras M, et al. Effects of Albumin Treatment on Systemic and Portal Hemodynamics and Systemic Inflammation in Patients With Decompensated Cirrhosis. Gastroenterology 2019;157:149-162.

11. Köberlin MS, Snijder B, Heinz LX, Baumann CL, Fauster A, Vladimer GI, et al. A Conserved Circular Network of Coregulated Lipids Modulates Innate Immune Responses. Cell 2015;162:170-183.

12. Hannun YA, Obeid LM. Sphingolipids and their metabolism in physiology and disease. Nat Rev Mol Cell Biol. 2018;19:175-191.

13. Cartier A, Hla T. Sphingosine 1-phosphate: Lipid signaling in pathology and therapy. Science 2019;366:eaar5551.

Journal Pre-proof

14. McPhail MJW, Shawcross DL, Lewis MR, Coltart I, Want EJ, Antoniades CG, et al. Multivariate metabotyping of plasma predicts survival in patients with decompensated cirrhosis. J Hepatol. 2016;64:1058-1067.

15. Grammatikos G, Ferreiròs N, Waidmann O, Bon D, Schroeter S, Koch A, et al. Serum Sphingolipid Variations Associate with Hepatic Decompensation and Survival in Patients with Cirrhosis. PLoS One 2015;10:e0138130

16. Becker S, Kinny-Köster B, Bartels M, Scholz M, Seehofer D, Berg T, et al. Low sphingosine-1-phosphate plasma levels are predictive for increased mortality in patients with liver cirrhosis. PLoS One 2017;12:e0174424.

17. Bernardi M, Angeli P, Clària J, Moreau R, Gines P, Jalan R, et al. Albumin in decompensated cirrhosis: new concepts and perspectives. Gut 2020;69:1127-1138.

18. Eisenberg S, Levy RI. Lipoprotein metabolism. Adv Lipid Res. 1975;13:1-89.

19. Loria P, Marchesini G, Nascimbeni F, Ballestri S, Maurantonio M, Carubbi F, et al. Cardiovascular risk, lipidemic phenotype and steatosis. A comparative analysis of cirrhotic and non-cirrhotic liver disease due to varying etiology. Atherosclerosis 2014;232:99-109.

20. Alarcon-Barrera JC, von Hegedus JH, Brouwers H, Steenvoorden E, Ioan-Facsinay A, Mayboroda OA, et al. Lipid metabolism of leukocytes in the unstimulated and activated states. Anal Bioanal Chem. 2020;412:2353-2363.

21. Rachakonda V, Argemi J, Borhani AA, Bataller R, Tevar A, Behari J. Reduced Serum Sphingolipids Constitute a Molecular Signature of Malnutrition in Hospitalized Patients With Decompensated Cirrhosis. Clin Transl Gastroenterol. 2019;10:e00013.

22. Sehrawat TS, Arab JP, Liu M, Amrollahi P, Wan M, Fan J, et al. Circulating extracellular vesicles carrying sphingolipid cargo for the diagnosis and dynamic risk profiling of alcoholic hepatitis. Hepatology 2021;73:571-585.

23. Hammad SM, Pierce JS, Soodavar F, Smith KJ, Al Gadban M, Rembiesa B, et al. Blood sphingolipidomics in healthy humans: impact of sample collection methodology. J Lipid Res. 2010;51:3074-87.

24. Trieb M, Rainer F, Stadlbauer V, Douschan P, Horvath A, Binder L, et al. HDL-related biomarkers are robust predictors of survival in patients with chronic liver failure. J Hepatol. 2020;73:113-120.

25. Kraemer FB, Khor VK, Shen WJ, Azhar S. Cholesterol ester droplets and steroidogenesis. Mol Cell Endocrinol. 2013;371:15-19.

26. Acevedo J, Fernández J, Prado V, Silva A, Castro M, Pavesi M, et al. Relative adrenal insufficiency in decompensated cirrhosis: Relationship to short-term risk of severe sepsis, hepatorenal syndrome, and death. Hepatology 2013;58:1757-65.

Journal Pre-proof

27. Elsbach P, Levy S. Increased synthesis of phospholipid during phagocytosis. J Clin Invest. 1968;47:2217-29.

28. Yan JJ, Jung JS, Lee JE, Lee J, Huh SO, Kim HS, et al. Therapeutic effects of lysophosphatidylcholine in experimental sepsis. Nat Med. 2004;10:161-167.

29. Murch O, Collin M, Sepodes B, Foster SJ, Mota-Filipe H, Thiemermann C. Lysophosphatidylcholine reduces the organ injury and dysfunction in rodent models of gramnegative and gram-positive shock. Br J Pharmacol. 2006;148:769-777.

30. Chen VL, Chen Y, Du X, Handelman SK, Speliotes EK. Genetic variants that associate with cirrhosis have pleiotropic effects on human traits. Liver Int. 2020;40:405-415.

31. Mann JP, Pietzner M, Wittemans LB, Rolfe EL, Kerrison ND, Imamura F, et al. Insights into genetic variants associated with NASH-fibrosis from metabolite profiling. Hum Mol Genet. 2020;29:3451-3463.

Journal Pre-proof

Figure Legends

Figure 1. Changes in blood lipids parallel disease severity.

(A) Supervised two-way clustering analysis of the lipid species across the four study groups (HS: healthy subjects, CC: patients with compensated cirrhosis, AD-no ACLF: patients with decompensated cirrhosis without acute-on-chronic liver failure (ACLF), AD-ACLF: patients with AD and ACLF). **(B)** Cleveland plot of the whole set of 223 annotated lipids ranked according to their fold changes between CC, AD-no ACLF and AD-ACLF vs. HS. Upper right inset: zooming in on the 15 lipids more abundant in AD-ACLF and AD-no ACLF in comparison to HS. Lower right inset: zooming on the 15 lipids with the highest fold change reductions in AD-ACLF and AD-no ACLF in comparison to HS. **(C)** Volcano plots of each lipid family in CC (top), AD-no ACLF (middle) and AD-ACLF (bottom) patients with respect to HS. Color coding on the left represents the different lipid families. **(D)** Supervised correlation matrix of blood lipid, non-lipid metabolites and cytokines/chemokines/macrophage markers within patients with cirrhosis at any disease stage.

Figure 2. Identification of a unique lipid fingerprint specific for AD-no ACLF.

(A) Unsupervised hierarchical cluster analysis of the area under the receiver-operating-characteristic curve (AUCs) assessing the discriminating accuracy of each of the 223 lipids in differentiating AD-no ACLF (left column) and AD-no ACLF without any organ dysfunction (mere AD-no ACLF) (right column) from CC patients. The 55 lipids composing cluster 1 are shown on the right. **(B)** Eigenlipid of the 55-lipid cluster across different groups, including HS and CC and AD-no ACLF patients. **(C)** Corresponding AUC values in assessing single liver dysfunction, liver failure or coagulation failure relative to mere AD-no ACLF. The AUC values in AD-no ACLF patients with and without bacterial infection relative to "mere AD-no ACLF" are also shown. **(D)** Eigenlipid of the 55-lipid cluster across four groups: AD-no ACLF without

any organ failure/dysfunction, single liver dysfunction, liver failure or coagulation failure. **(E)** Eigenlipid of the 55 lipid fingerprint in AD-no ACLF patients with bacterial infection and in those without.

Figure 3. The sphingomyelin landscape in AD-no ACLF.

(A) Schematic diagram of the sphingolipid pathway. *De novo* sphingolipid biosynthesis in the endoplasmic reticulum involves the condensation of L-serine with palmitoyl-CoA mediated by the enzyme serine palmitoyltransferase 1 (SPTLC1) to produce ceramide, which is then transported to the Golgi for the synthesis of **sphingomyelin (**SM). Alternatively, SM can be synthesized in the Golgi from phosphatidylcholine (PC) and ceramide by SM synthase 1 (SGMS1). SM breakdown to ceramide is catalyzed by acid sphingomyelinase (SMPD1). Ceramide can be converted into sphingosine-1-phosphate, which is catabolically converted into *trans*-2-hexadecenal and phosphoethanolamine though the action of the enzyme S1P lyase (SGPL1). **(B-G)** Serum levels of SM(d18:1/21:1) and SM(d18:1/23:0), PC(37:3), serine, palmitate, choline and Cer(d18:1/C22:0) across the four study groups (HS: healthy subjects, CC: patients with compensated cirrhosis, AD: patients with acutely decompensated cirrhosis without ACLF, ACLF: patients with acutely decompensated cirrhosis with ACLF). **(H)** Serum levels of sphingosine-1-phosphate in HS and in a subgroup of 80 patients with AD cirrhosis with and without ACLF. **(I)** Expression of the genes *SPLTC1*, *SGMS1*, *SMPD1* and *SGPL1* in peripheral blood mononuclear cells isolated from 10 HS, 4 patients with CC, 11 with AD without ACLF and 11 with AD and ACLF.

Figure 4. Identification of a distinct lipid fingerprint specific for AD-ACLF.

(A) Unsupervised hierarchical cluster analysis of AUCs assessing the discriminating accuracy of each of the 223 lipids in differentiating AD-ACLF of any grade from mere AD-no ACLF

Journal Pre-proof

(first column) and AD-ACLF-1, -2, and -3 relative to mere AD-no ACLF (second, third and fourth columns, respectively). **(B)** Eigenlipid of the 17-lipid cluster (see text for details) across different groups, including HS and patients with CC, AD-no ACLF and patients with AD-ACLF. **(C)** Eigenlipid of the 17-lipid cluster across mere AD-no ACLF and AD-ACLF grades (AD-ACLF-1, AD-ACLF-2 and AD-ACLF-3). **(D)** Corresponding lipid AUC values in discriminating patients with single kidney failure or dysfunction (second column), patients with single liver failure associated with kidney and/or brain dysfunction (third column), and patients with liver failure combined with either kidney, brain or coagulation failures (fourth, fifth and sixth) relative to AD-no ACLF without any organ failure/dysfunction (patients with "mere AD". **(E)** Corresponding lipid AUC values in discriminating AD-ACLF patients with bacterial infection from those without. In the graphs, the AD-ACLF group is abbreviated as ACLF.

Figure 5. The cholesteryl ester (CE) and lysophosphatidylcholine (LPC) landscape in AD-ACLF.

(A) Serum levels of CE(16:0) and CE(18:3) across the four study groups (HS: healthy subjects, CC: patients with compensated cirrhosis, AD: patients with acutely decompensated cirrhosis without ACLF, ACLF: patients with acutely decompensated cirrhosis and ACLF). **(B)** Schematic diagram of CE biosynthesis. CEs are synthesized by the enzyme lecithin-cholesterol acyl transferase (LCAT), which transfers a fatty acid (FA) from position sn-2 of phosphatidylcholine (PC) to cholesterol, particularly on the surface of high-density lipoproteins (HDL). The removal of a FA from PC by LCAT results in the formation of LPC. **(C)** Plasma levels of LCAT in the four groups of study. **(D)** PC to LPC ratio in the four study groups.

Figure 6. Dynamics of the AD-no ACLF and AD-ACLF lipid fingerprints. The dynamics of the specific AD-no ACLF and AD-ACLF lipid fingerprints were investigated in the

validation cohort including 265 patients who underwent the 28-day follow-up. **(A)** Unsupervised hierarchical cluster analysis of the area under the receiver-operating-characteristic curve (AUCs) in patients with AD-no ACLF whose condition worsened. **(B)** Unsupervised hierarchical cluster analysis of lipid AUCs in patients with AD-ACLF whose condition improved. (**C)** Eigenlipid of the AD-no ACLF fingerprint according to 28-day mortality. **(D)** Eigenlipid of the AD-ACLF fingerprint according to 28-day mortality. **(E)** Heatmap of the 27 metabolites that changed levels after receiving standard medical therapy (SMT) alone (n=41) or SMT+HSA therapy (n=37). **(F)** Levels of LPC(O-16:0) before (day 0) and after (3 and 7 days) receiving SMT alone or SMT+HSA therapy. (**G**) Levels of LPC(O-16:0) in patients of the validation cohort whose clinical status improved (left graph) or who survived the 28-day follow-up (right graph).

Journal Pre-proof

Table 1: Baseline characteristics and markers of systemic inflammation in patients with compensated cirrhosis and patients with acutely decompensated (AD) cirrhosis without ACLF (AD-no ACLF) and those with ACLF (AD-ACLF) included in the discovery cohort.

Variable	Compensated cirrhosis n= 43	AD-no ACLF n= 518	AD-ACLF n= 43
Age (Years)	61 ± 8.78	58.22 ± 12.09	60.70 ± 10.74
Gender (Male)	15 (75%)	333 (64.29%)	30 (69.77%)
Cirrhosis Etiology			
Alcohol	9 (21.0%)	229 (44.21%)**	27 (62.79%)
HCV	19 (44.2%)	114 (22.01%)**	12 (27.91%)
Alcohol+HCV	0 (0%)	51 (9.85%)*	2(4.65%)
Other	15 (34.8%)	89 (17.18%)*	1 (2.33)[a]
Decompensations at Inclusion			
Ascites or surrogates[1]	-	301 (58.11%)	24 (55.81%)
Encephalopathy	-	137 (26.45%)	27 (62.79%)[c]
Bacterial infection	-	101 (19.50%)	14(32.56%)
GI-Bleeding	-	86 (16.60%)	6 (13.95%)
Laboratory data			
Serum bilirubin (mg/dL)	1.08 ± 0.76	4.48 ± 5.44***	11.96 ± 12.89[c]
Serum creatinine (mg/dL)	0.86 ± 0.28	0.96 ± 0.37	2.44 ± 1.58[c]
C-reactive protein (mg/L)	3.80 ± 4.18	24.52 ± 28.01***	35.88 ± 33.12[b]
INR	1.2 ± 0.42	1.51 ± 0.39***	1.89 ± 0.73[c]
Serum albumin (g/dL)	4.01 ± 0.47	2.96 ± 0.60***	2.90 ± 0.68
WBC count (x10^9cells/L)	5.76 ± 2.32	6.60 ± 4.11	9.97 ± 6.32[c]
TNFα (pg/mL)	6.45 ± 4.69	23.27 ± 14.10***	32.27 ± 34.66[a]
IL-6 (pg/mL)	2.00 ± 3.11	45.84 ± 105.51**	250.08 ± 824.16[c]
IL-8 (pg/mL)	6.65 ± 4.12	88.61 ± 136.91***	112.48 ± 107.39[b]

HCV: hepatitis C virus; INR: international normalized ratio; WBC: white blood cell; TNF: tumor necrosis factor; IL: interleukin.
[1]Surrogates of ascites: paracentesis. spontaneous bacterial peritonitis. diuretic treatment or transjugular intrahepatic portosystemic shunt (TIPS) for ascites prior to enrolment.
*p<0.05. **p<0.01 and ***p<0.001 for AD-no ACLF vs compensated cirrhosis; [a]p<0.05. [b]p<0.01 and [c]p<0.001 for AD-ACLF vs AD-no ACLF.

Journal Pre-proof

Figure 1

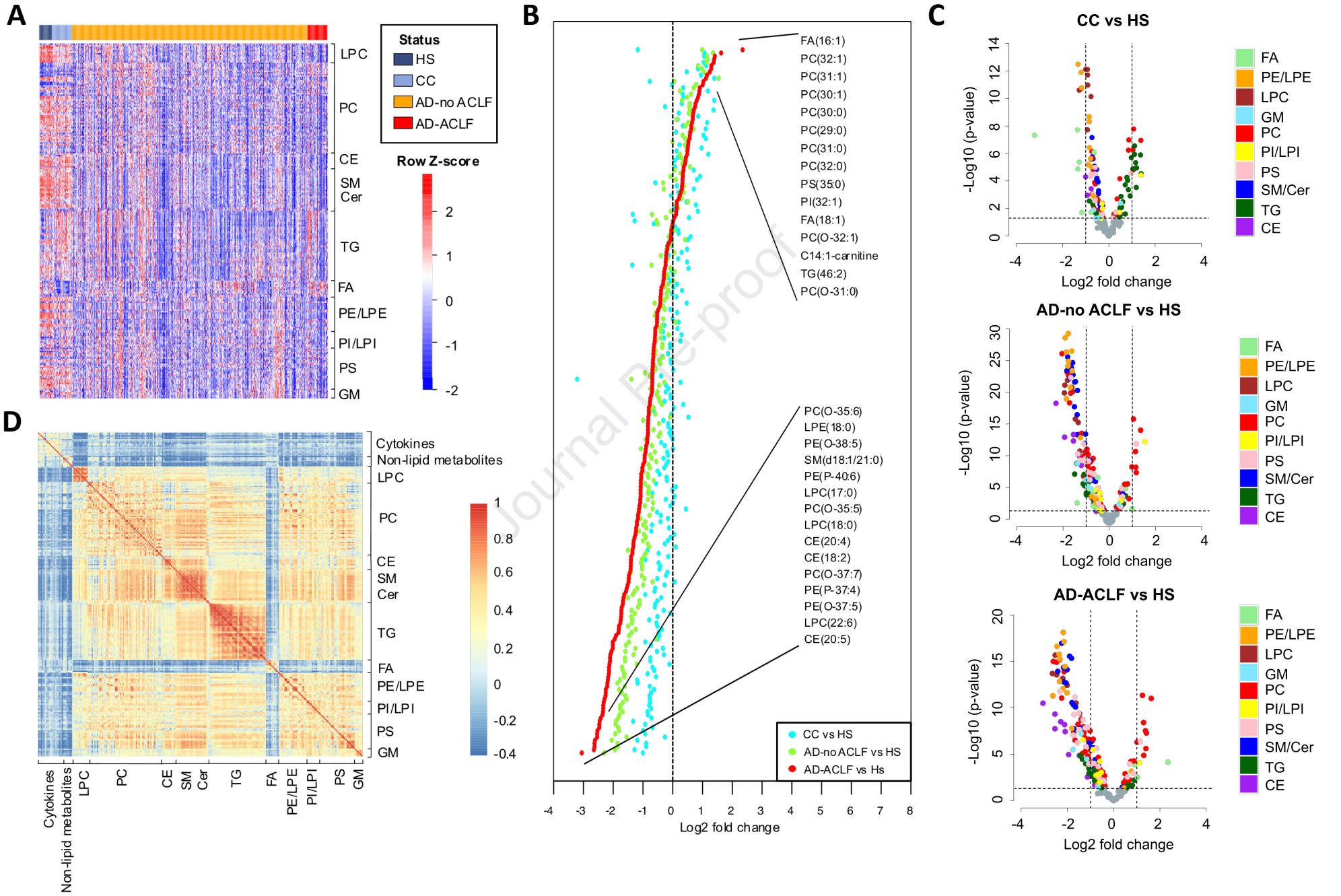

Journal Pre-proof

Figure 2

Journal Pre-proof

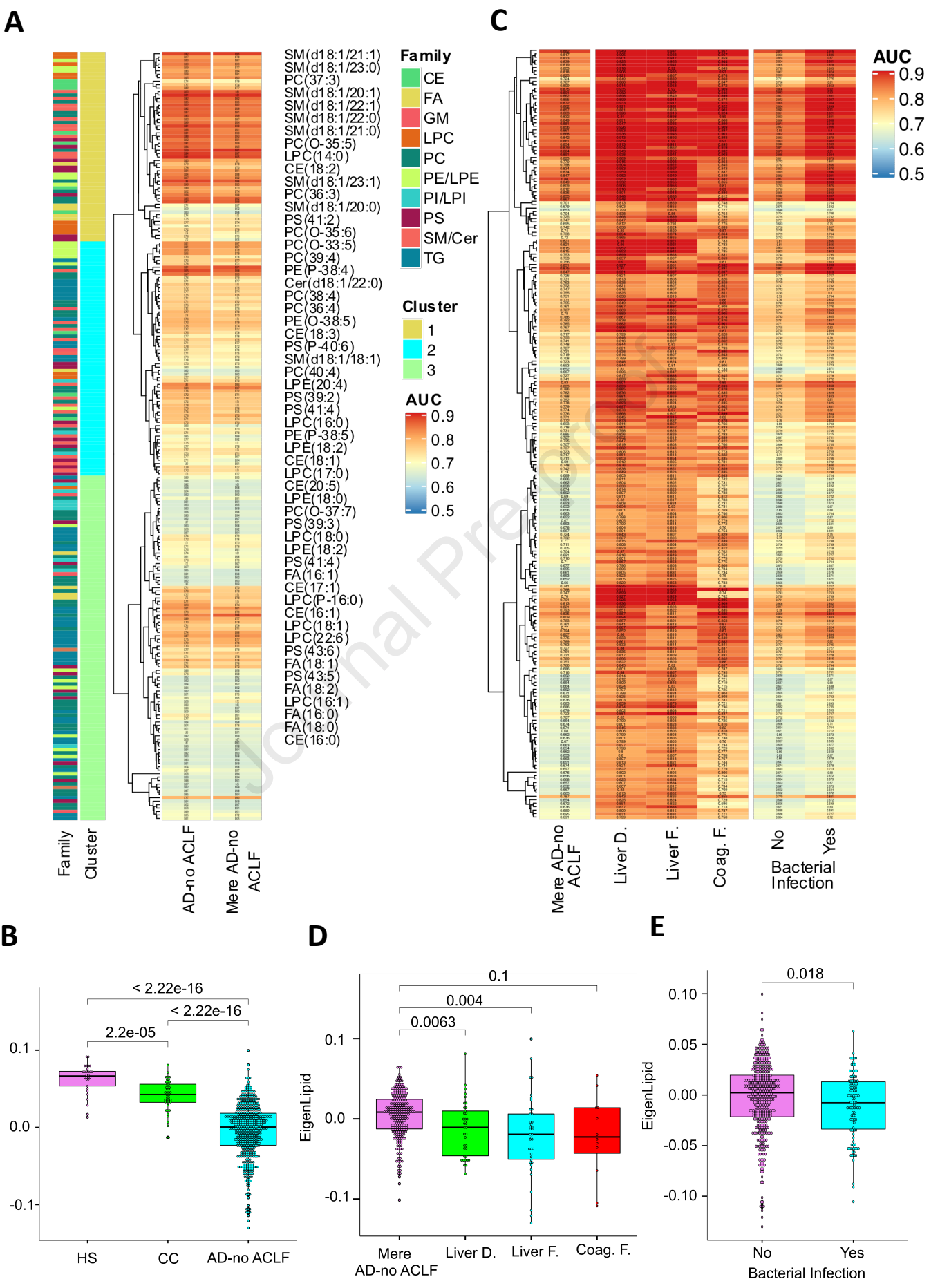

Figure 3

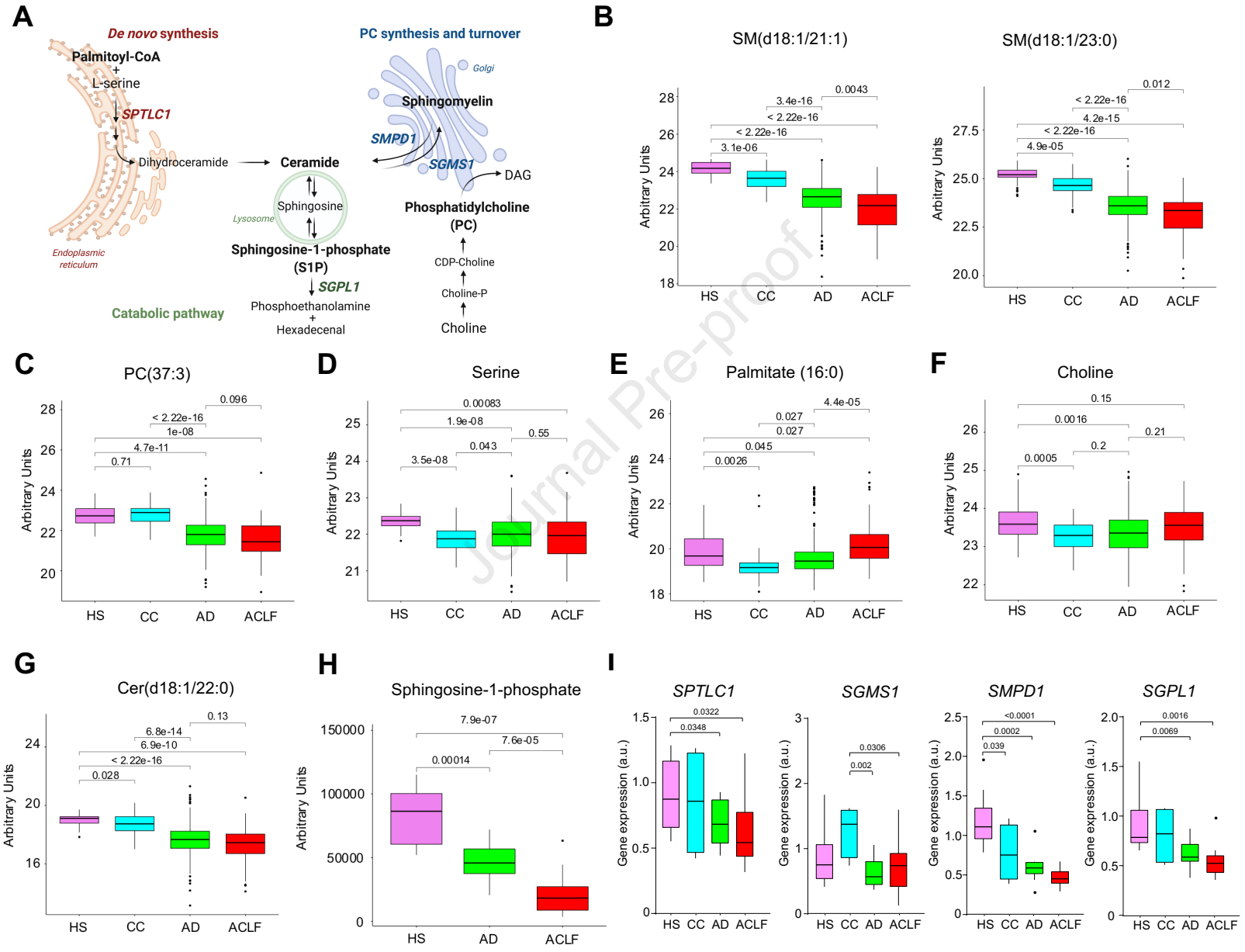
A
De novo synthesis
Palmitoyl-CoA
+
L-serine
SPTLC1
Dihydroceramide
Ceramide
Sphingosine
Lysosome
Sphingosine-1-phosphate
(S1P)
SGPL1
Phosphoethanolamine
+
Hexadecenal
Endoplasmic reticulum
Catabolic pathway
PC synthesis and turnover
Golgi
Sphingomyelin
SMPD1
SGMS1
DAG
Phosphatidylcholine
(PC)
CDP-Choline
Choline-P
Choline
B
SM(d18:1/21:1)
SM(d18:1/23:0)
Arbitrary Units
HS CC AD ACLF
C
PC(37:3)
D
Serine
E
Palmitate (16:0)
F
Choline
G
Cer(d18:1/22:0)
H
Sphingosine-1-phosphate
I
SPTLC1
SGMS1
SMPD1
SGPL1
Gene expression (a.u.)

Journal Pre-proof

Figure 4

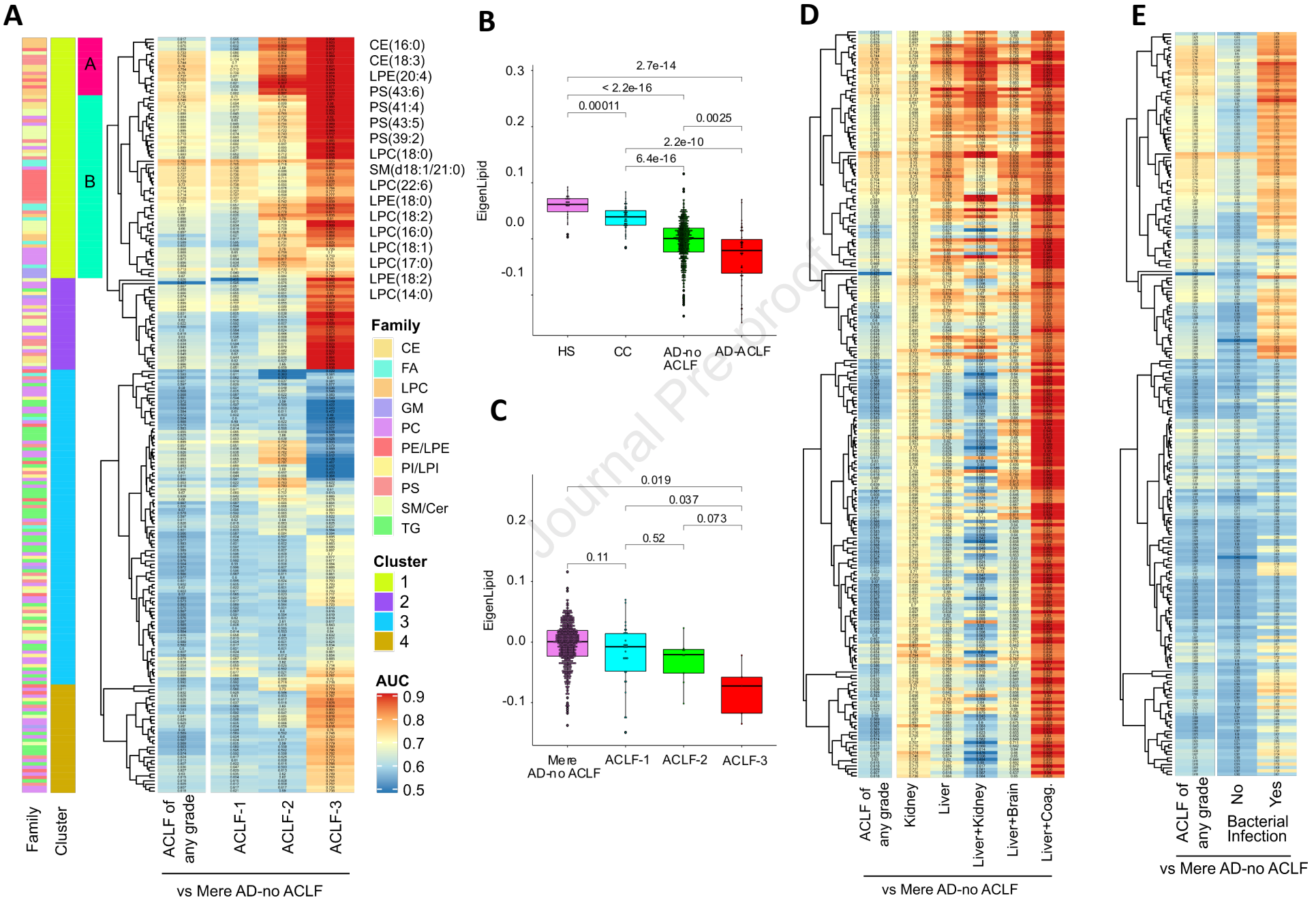

Figure 5

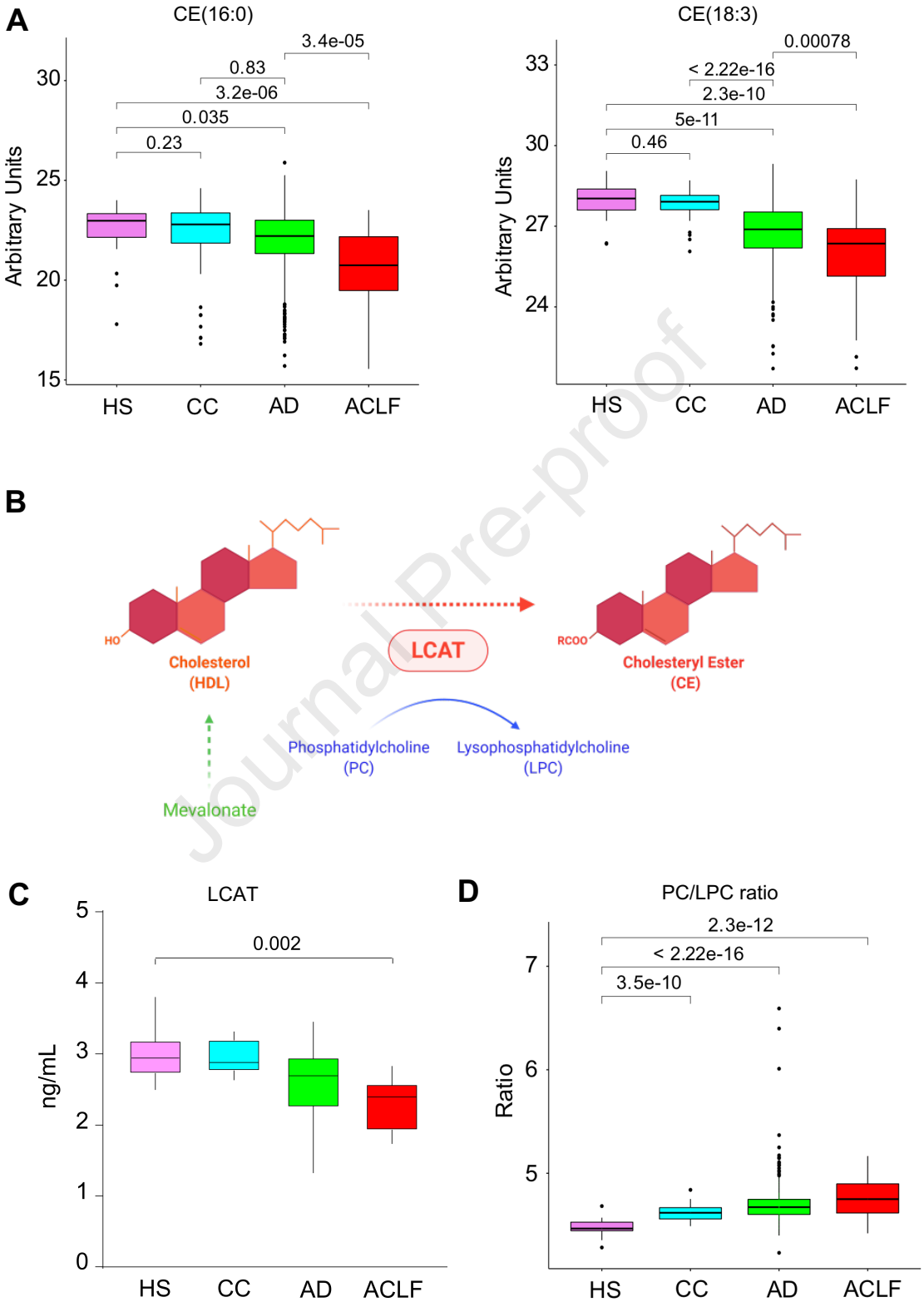

Journal Pre-proof

Figure 6

Journal Pre-proof

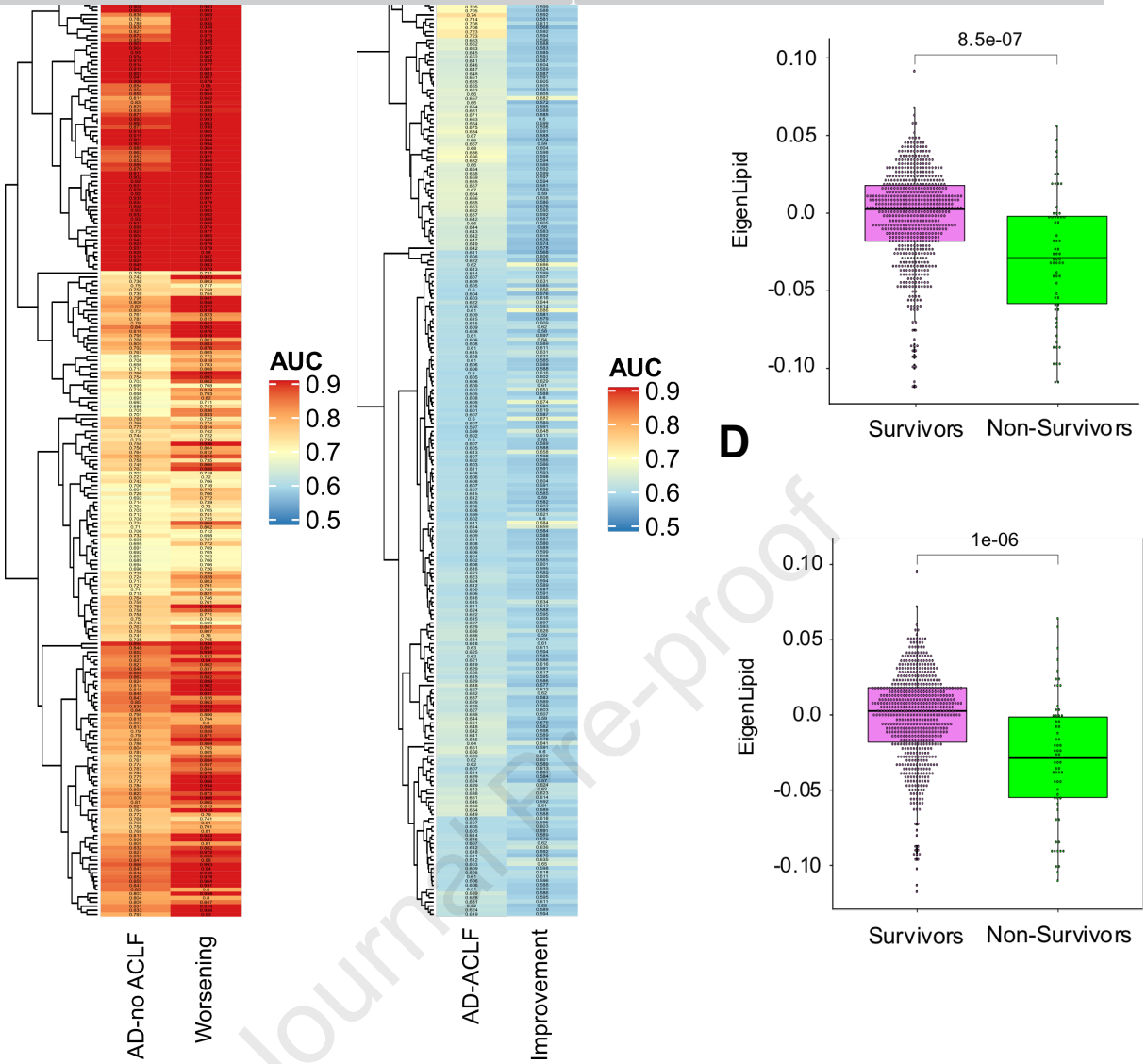

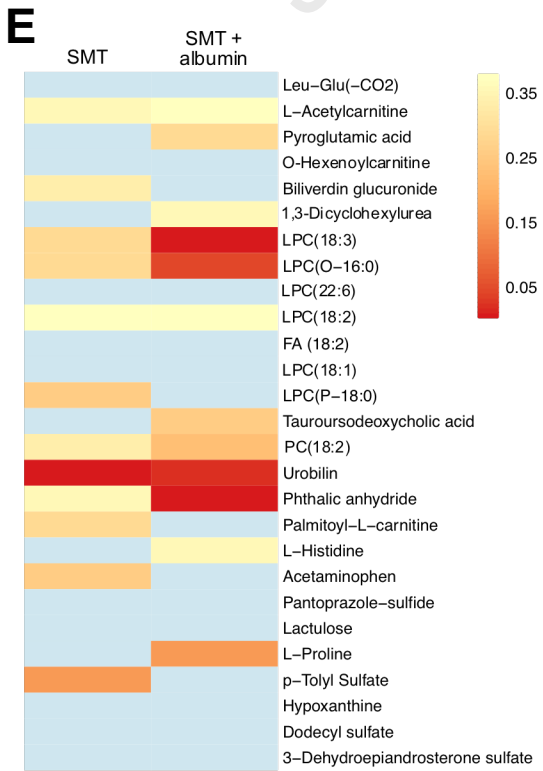

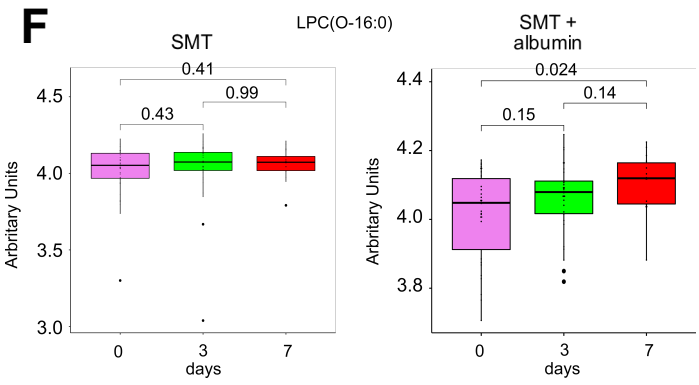

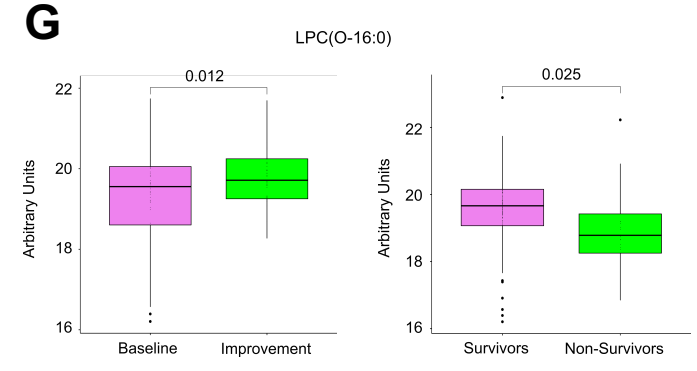

Journal Pre-proof

Highlights

- The blood lipidome of patients with acutely decompensated (AD) cirrhosis with and without ACLF was characterized by untargeted lipidomics.
- The characteristic lipid landscape of AD cirrhosis and ACLF was a generalized suppression of all lipid families except fatty acids.
- Liver dysfunction was the principal net contributor to this landscape.
- Sphingomyelins showed discriminating accuracy for AD cirrhosis whereas cholesteryl esters and lysophosphatidylcholines discriminated ACLF.
- Restoration of lysophosphatidylcholine levels was observed in patients receiving albumin therapy.

Journal Pre-proof